Estimation of Friction Power during Manual Wheelchair Propulsion using Inertial Measurements Units

N.C. van Dam

Delft University of Technology

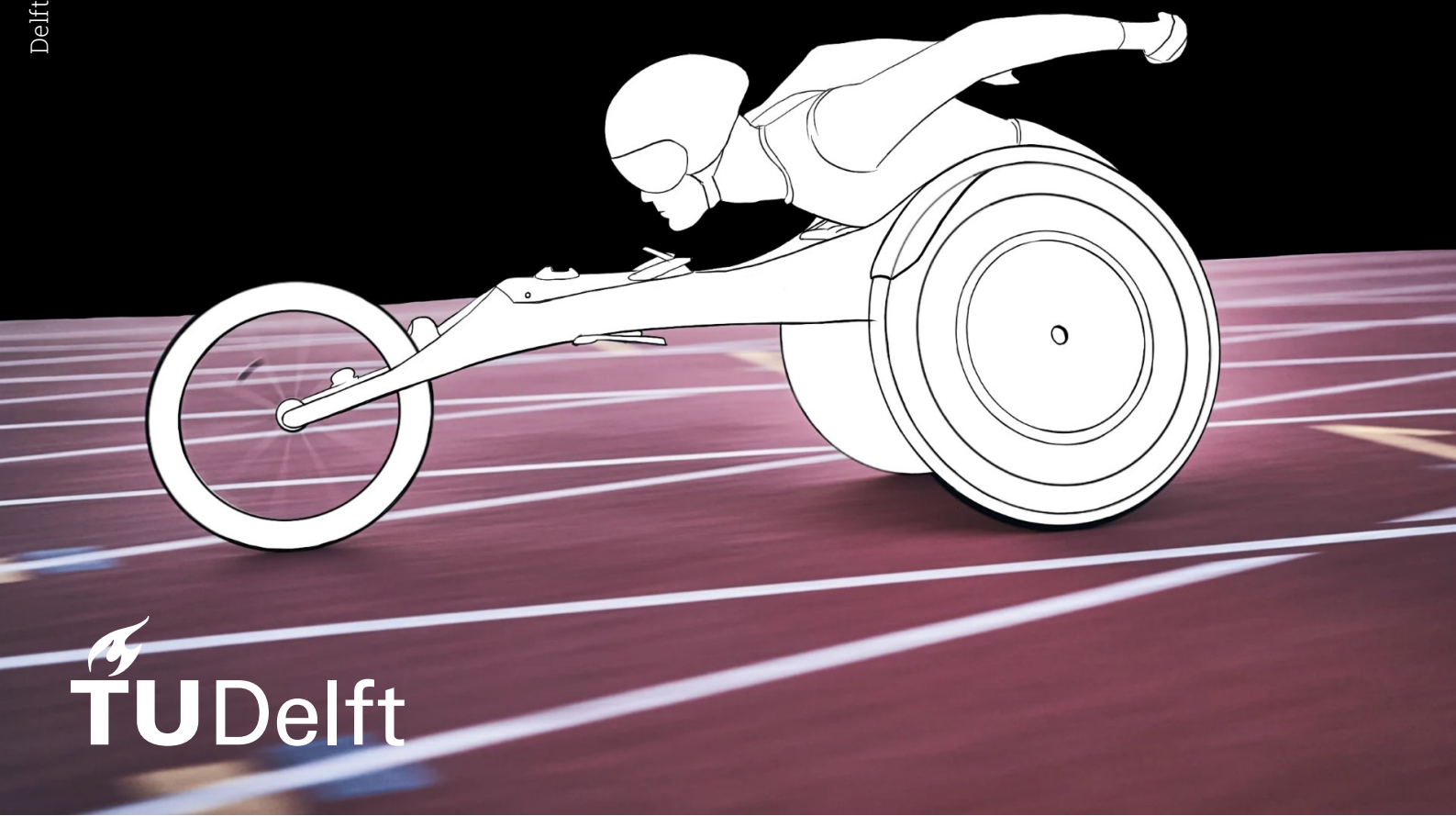

TU Delft

Estimation of Friction Power during Manual Wheelchair Propulsion using Inertial Measurements Units

by

N.C. van Dam

to obtain the degree of Master of Science
at the Delft University of Technology
to be defended publicly on July 21, 2023 at 10:00.

Msc Mechanical Engineering
Track: Biomechanical Design
Specialisation: Bio Robotics

Student number: 4484975
Project duration: September, 2023 - July, 2023
Thesis committee: Prof.dr. H.E.J. Veeger (Supervisor)
M.P. van Dijk, MSc (Supervisor)
Prof.dr.ir. A.C. Schouten

TU Delft

Estimation of Friction Power during Manual Wheelchair Propulsion using Inertial Measurement Units

N.C. van Dam

Abstract

Propulsion power is an important metric in wheelchair racing. For a flat surface, it can be estimated from the sum of friction power and kinetic power. Usually, to determine friction power, the rolling and air drag coefficient first need to be determined with coast-down tests or other time-consuming methods. The aim of this paper was to investigate whether friction power could be estimated from Inertial Measurement Unit (IMU) data during wheelchair propulsion without the need for previously determining these coefficients. Two approaches were investigated using the kinematic data of a wheelchair athlete measured by a wheel, frame and trunk IMU. Firstly, an approach was used that considers the recovery phase of the propulsion cycle to be a coast-down period. Secondly, a machine-learning approach (Random Forest Regressor) was implemented. Coast-down tests were used to calculate a reference power with which the results from the two approaches could be compared. Results indicate that the machine-learning approach is more promising than the recovery phase analysis. However, whether the current machine-learning model can predict friction power for unseen subjects and surfaces should still be determined with inter-subject validation. Otherwise, it is recommended that a machine-learning model is trained for multiple subjects and a variation in conditions affecting friction force (surface, tyre pressure, wind, slope) to achieve a more robust model.

I. Introduction

Mechanical power is an important metric in endurance sports. Because mechanical power is less sensitive to variations in environmental variables such as wind, slope and road conditions, it can be used as an objective measurement to assess an athlete's performance [1]. On top of this, it can be used to monitor fitness and fatigue, and to assess training load [2]. Consequently, it can play an important role for coaches and athletes in training and game preparation [3].

However, in wheelchair racing, determining mechanical power is challenging. One way to determine it is by measuring the forces and moments on the hand rim directly and multiplying these with the linear and angular velocities of their point of application. However, this requires an instrumented wheel. Such a wheel adds mass to the system, which is undesirable as this significantly influences performance [3]. Moreover, only a few instrumented wheels exist [4]. Therefore, mechanical power is often estimated via the resistive forces by solving the power equation [5].

The power equation can be deducted from the Free Body Diagram in Figure 1 and can be expressed as [6], [7]:

$$\begin{aligned} P_{\mathrm{p}} &= P_{\mathrm{f}} + P_{\mathrm{g}} + P_{\mathrm{kin}} \\ &= (F_{\mathrm{roll}} + F_{\mathrm{air}} + F_{\mathrm{int}} + mg\sin(\alpha) + ma)v \end{aligned} \tag{1}$$

where N is the normal force, F_{roll} is the rolling resistance, F_{air} is the air resistance, F_{int} is the internal friction, m is the mass of the wheelchair-athlete combination, g is the gravitational constant, α is the angle of slope and a and v are the linear acceleration and velocity of the

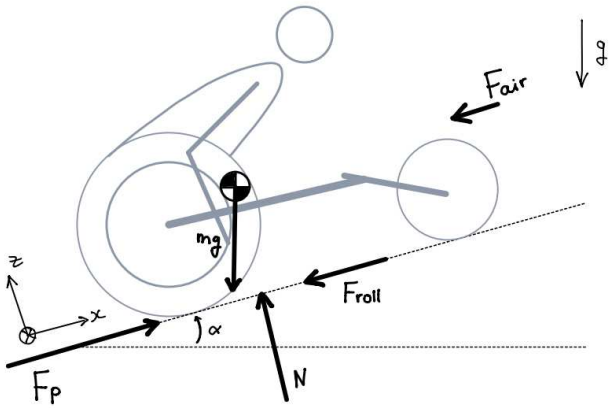

Fig. 1: Free body diagram of a wheelchair and athlete

wheelchair, respectively. According to the power equation, the mechanical power produced by the athlete to propel the wheelchair (P_{p}) is equal to the sum of the friction power due to rolling and air resistance (P_{f}), the kinetic power (P_{kin}), and the gravitational power which is present when wheeling on a slope (P_{g}). In other words, the propulsion power due to the propulsion force that is applied to the hand rims by the athlete (F_{p}) is used to overcome power losses due to resistive forces which results in an acceleration of the wheelchair [5]. Thus, in order to determine the propulsion power, the friction forces and power need to be determined.

Most methods that are described in the literature to determine the friction forces and power require the previous estimation of the rolling and air resistance coefficient for the specific wheelchair-athlete combination and the relevant surface [1], [3], [8]–[13]. The available methods to determine these coefficients include drag tests, Computational Fluid Dynamics (CFD) software and coast-down tests. However, these procedures are time-intensive. Moreover, in para-triathlons and marathons, multiple surfaces and/or wind conditions might be encountered during one race. In that case, the coefficients would have to be determined for each specific condition. Therefore, a method which can directly determine the friction power during propulsion without the previous determination of these coefficients would be preferable.

During a coast-down test, the wheelchair is accelerated to a certain speed, after which the athlete sits as still as possible in a racing position while the wheelchair decelerates. Since there is no propulsion force, the total friction force can be calculated by multiplying the mass by the deceleration of the wheelchair ($F_{\mathrm{friction}} = ma$).

During the recovery phase of the propulsion cycle, the athlete does not apply any force to the hand rims. Therefore, the recovery phase can be considered a short coast-down period and similar to a coast-down test, the total friction force can be calculated from ma. Rietveld et al. [3] have done research on this. They used line-fitting to velocity data from Inertial Measurement Units (IMUs) from sprint tests to determine the deceleration in the recovery phases. However, they did not succeed in performing power prediction using this method and recommended further research.

The aim of this paper was to investigate whether friction power could be estimated from IMU data without the need for previously determining the rolling and air resistance coefficients. Two approaches to achieve this goal were investigated. Firstly, the approach by Rietveld et al. [3] was further investigated, in which the recovery phase of the propulsion cycle is considered a coast-down period. Secondly, a machine-learning approach was implemented to try and estimate the friction power directly from IMU propulsion data.

II. Methods

A. Experimental procedure

One subject (male, 75 kg) participated in this study. He used a racing wheelchair with a mass of $10.5\,\mathrm{kg}$, a camber angle of $0.18\,\mathrm{rad}$, a rear wheel diameter of $67\,\mathrm{cm}$, a front wheel diameter of $47\,\mathrm{cm}$, a wheel base of $61\,\mathrm{cm}$ and a tyre pressure of 6 and $7\,\mathrm{bar}$ of the left and right tyre, respectively. The tests were performed on an outdoor athletic track in Papendal in the Netherlands. The study was approved by the Human Research Ethics Committee of the Technical University of Delft. Prior to the experiment, the participant gave informed consent.

Firstly, two sets of coast-down tests were performed on the athletic track: for the first set, the subject completed three pushes before coasting and for the second set the subject was instructed to complete 10 pushes before coasting to achieve a higher velocity. For each set, the coast-down test was performed two times in both directions, so four times in total. During the coast-down test, the subject was instructed to sit in a racing position while remaining as still as possible.

Secondly, the subject executed a series of propulsion tasks on the athletic track. The subject was first instructed to do two sets at a relaxed pace with rest in between (relaxed-pace). Then the subject was instructed to perform three sprints in succession (sprints). Finally, the subject performed 5 sets of 800 m, in which the first 250m were at a fast pace, the following 300m at a slower pace and the final 250m at a fast pace again (fast-pace).

B. Equipment

Three IMUs (MoveSense, Suunto Oy, Vantaa, Finland) were used to collect 3D inertial sensor data. The IMUs were placed on the axis of the right rear wheel, on the wheelchair frame and on the trunk of the athlete. The IMU on the wheel and frame had a sampling frequency of $100\,\mathrm{Hz}$ and provided gyroscope data. The IMU on the trunk had a sampling frequency of $50\,\mathrm{Hz}$ and provided both gyroscope and accelerometer data. The IMU data were collected via Wi-Fi using the wheelchair mobility performance monitor (WMPM) app [14], which automatically synchronised the time between the sensors.

C. Pre-processing

All IMU data were imported and processed in Python (version 3.8.5, Python Software Foundation, Wilmington, DE, United States). All data were resampled to a sampling frequency of $50\,\mathrm{Hz}$ using linear interpolation. The gyroscope signal of the frame IMU around its vertical axis was low-pass filtered with a recursive Butterworth filter with a cut-off frequency of $0.2\,\mathrm{Hz}$. All other IMU data were low-pass filtered with a recursive Butterworth filter with a cut-off frequency of $10\,\mathrm{Hz}$ [15].

To determine the linear wheelchair velocity (v), a series of transformations were applied to the IMU data. Because of the wheel camber, the angular wheel velocity measured by the wheel IMU

around the wheel axis (ω_{wheel}) is affected by frame rotations [16]. Accordingly, the measured angular wheel velocity was corrected for frame rotations with the use of the frame angular velocity (ω_{frame}) measured by the frame gyroscope around its vertical axis, using Equation 2. From the corrected angular wheel velocity ($\omega_{\text{wheel, corrected}}$), the wheel linear velocity (v_{wheel}) and finally, the linear wheelchair velocity (v) were determined using Equation 3, 4 and 5.

$$\omega_{\text{wheel, corrected}} = \omega_{\text{wheel}} - \omega_{\text{frame}} \sin(\varphi_{\text{camber}}) \tag{2}$$

$$v_{\text{wheel}} = \frac{\omega_{\text{wheel}} D \pi}{360} \tag{3}$$

$$d_{\text{axle,centre}} = WB/2 - \sin(\varphi_{\text{camber}}) 0.5D \tag{4}$$

$$v = v_{\text{wheel}} - (\tan(\omega_{\text{frame}}/fs) d_{\text{axle,centre}}) fs \tag{5}$$

In which, D is the wheel diameter, $d_{\text{axle,centre}}$ is the distance between the wheel axle and frame centre, WB is the wheelbase, φ_{camber} is the camber angle and fs is the sampling frequency. These equations are based on the approach described by van Dijk et al. [17].

The linear acceleration (a) of the wheelchair was determined by taking the derivative of the linear wheelchair velocity. The trunk angle was determined by combining the gyroscope and accelerometer data of the trunk, using the imufusion Python package which is based on an Attitude And Heading Reference System (AHRS) algorithm.

D. Data analysis

Coast-down tests: The coast-down tests were used to determine the rolling coefficient (μ_{R}) and the lumped drag coefficient ($C_{\text{D}}A$). Firstly, the coast-down areas were manually selected. Subsequently, non-linear least-square fitting was used to fit Equation 6 to the linear velocity data in the coast-down areas (see Figure 2) in order to determine c_1 and c_2 [13], [18]. The μ_{R} and $C_{\text{D}}A$ were determined using Equations 7 and 8, in which ρ is the air density. Lastly, the values for each coast-down test were averaged to get one final value for μ_R and $C_{\text{D}}A$. The mean deceleration was determined as well by fitting a line to the coast-down velocity data and finding the slope.

$$v = \sqrt{\frac{c_2}{c_1}} \tan\left[\tan^{-1}\left(v_0 \sqrt{\frac{c_1}{c_2}}\right) - t\frac{\sqrt{c_1 c_2}}{m}\right] \tag{6}$$

$$c_1 = \frac{\rho A C_{\text{D}}}{2} \tag{7}$$

$$c_2 = \mu_{\text{R}} m g \tag{8}$$

Reference power: The reference friction power was determined from Equations 9, 10 and 11 using the linear velocity data of the wheelchair and the constants determined in the coast-down tests.

$$P_{\text{f}} = (F_{\text{roll}} + F_{\text{air}}) v \tag{9}$$

$$F_{\text{roll}} = c_2 \tag{10}$$

$$F_{\text{air}} = c_1 v^2 \tag{11}$$

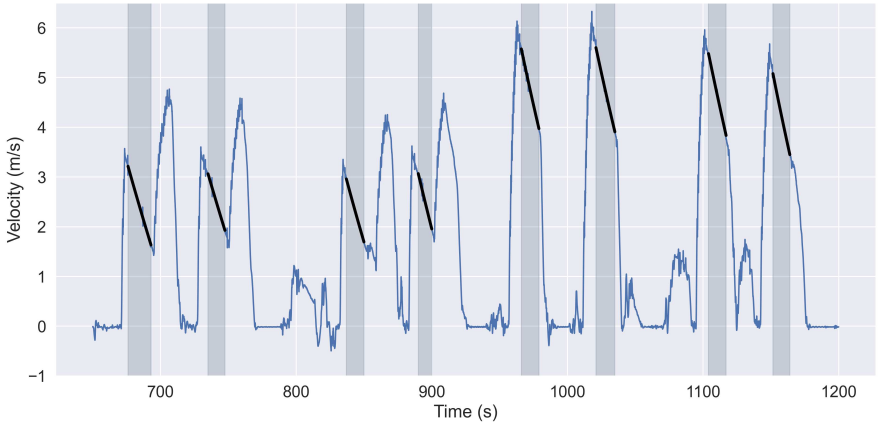

Fig. 2: Coast-down test velocity data with the non-linear least-square fit (black line). The grey areas represent the manually selected coast-down areas. The first four coast-down tests were performed after 3 pushes and the last four after 10 pushes.

Recovery phase analysis: An automated push-detection algorithm was used to identify the pushes. The main forward accelerations were considered to be pushes [19]. A frequency spectrum was made and the mean push frequency was assumed to be the most prominent frequency over 1.2 Hz and below 3.5 Hz. The linear acceleration was low-pass filtered with a low-pass recursive Butterworth filter with a cut-off frequency of 1.5 times this mean push frequency. Subsequently, acceleration peaks were identified using a minimal peak height and prominence of 1.2 times the standard deviation and a minimal peak distance of 0.83 times the assumed mean push frequency. In this way, only the large peaks were defined as pushes. From visual inspection, it became clear that two types of pushes could be distinguished: short and long pushes. Preliminary results showed that the recovery phases of the short pushes were too short to count as coast-down periods resulting in too high decelerations. Therefore, only the long pushes (at least 1 second long) were selected.

Subsequently, the coast-down periods were identified. The large peaks in the velocity signal corresponding to the long pushes were selected as the beginning of the coast-down period and were found using a minimal peak height of 0.3 times the standard deviation and prominence and a minimal peak distance of 20 times the mean frequency. To find the end of the coast-down period, a non-push detection algorithm was implemented. A non-push was defined as the final minimum in the acceleration before the subsequent push (see Figure 3). To find the non-pushes, a minimal peak height and prominence of 0.1 times the standard deviation, a peak distance of 0.83 times the mean frequency and a width of 2 times the standard deviation were used. Only the non-pushes following the long pushes were selected.

To improve the algorithm, faulty coast-down periods were removed by implementing an extra check that checks the distance between the beginning and end of the coast-down period. When the distance between these two was larger than 3 seconds or smaller than 0.6 seconds, the coast-down period was removed.

A line was fitted to the velocity signal for each coast-down period (see Figure 3). The slope of this line represents the deceleration in these areas. Deceleration values that were 2 times larger or 0.5 times smaller than the mean deceleration from the coast-down tests were removed

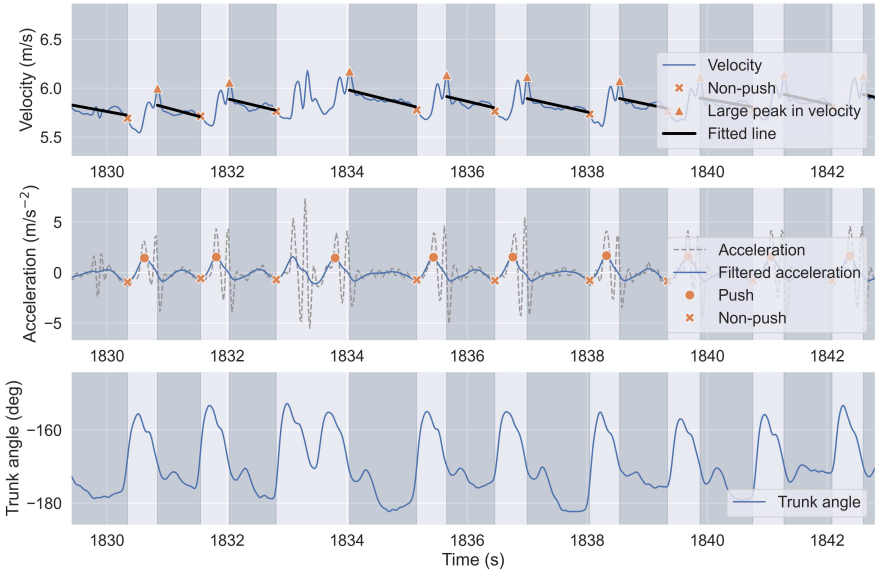

Fig. 3: Example of the linear velocity, acceleration and trunk angle signal with the selected pushes (orange dot), non-pushes (orange x) and large peaks in velocity (orange triangle). The black lines show the fit that is made by the automated algorithm in the selected coast-down periods (grey areas).

to remove unrealistic values. Thereafter, the deceleration was used to determine the total friction force using $F_\mathrm{f} = ma$. The rolling mean per 5 seconds was computed to produce a continuous friction force signal. The friction power was then calculated using Equation 12).

$$P_\mathrm{f} = F_\mathrm{f} v \tag{12}$$

To be able to distinguish between straights and turns on the track, the angular velocity of the frame around its vertical axis was used. Whenever it was higher than $6\,\mathrm{deg/s}$, this was considered a turn and when it was lower than this value, it was considered a straight. This threshold was chosen in such a way that the calculated distance on the straights (determined from the integration of the linear velocity) corresponded to the actual distance of the straights ($\sim 85\,\mathrm{m}$).

To evaluate this analysis, the predicted friction force and power were plotted against their reference value. Moreover, for the relaxed-pace and fast-pace propulsion sets, boxplots of the predicted and reference power were computed. In the boxplots, a division was made between the straights and turns. Since the predicted power is based on a rolling mean, the first and last values of the turns and straights are influenced by each other. Therefore, the first 3 and last 3 seconds of the turns and straights were removed before creating the boxplots.

Machine learning: The data were manually divided into a training and test set so that each type of propulsion task (relaxed-pace, sprints, fast-pace) was represented in both the training and test set. The last half of the second relaxed-speed propulsion, the last set of sprints and the last set of fast-pace propulsion were selected for the test set. The rest of the velocity signal was assigned to the training set (see Figure 4).

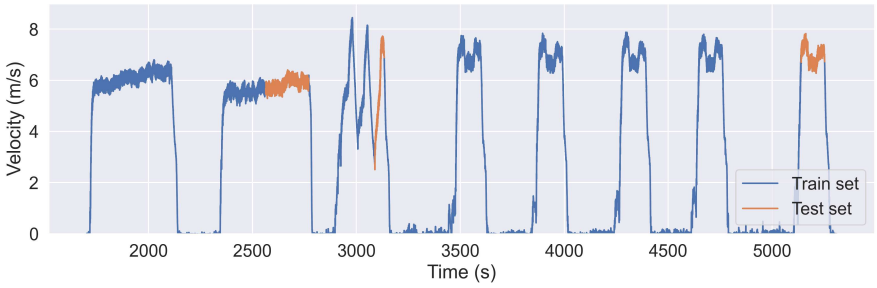

Fig. 4: Training and test set.

The velocity was chosen as a predictor feature since this signal was also used to determine the reference friction power. Using this feature, a machine-learning model was trained to predict friction power.

A Random Forest Regressor algorithm was employed to train and test the friction power prediction. Random forests are an ensemble of prediction trees which are trained in parallel. Each tree is trained based on a random part of the training set. The results of each tree are averaged to produce a single result [20]. All hyperparameters were set to their default values in Scikit-Learn. No hyperparameter tuning was performed since the model already worked sufficiently without.

To evaluate the performance of the model, the mean absolute error (MAE), root mean squared error (RMSE) and coefficient of determination (R2) were computed. To compare the performance for the different propulsion tasks, the performance metrics were computed separately for each propulsion task.

III. Results

A. Coast-down tests

The non-linear least-square fit resulted in a μ_R of 0.0102 ± 0.00101 and a $C_\mathrm{D}A$ of $0.136 \pm 0.0293\,\mathrm{m}^2$. The mean deceleration during the coast-down tests after performing three pushes (average velocity around $2.5\,\mathrm{m/s}$) and ten pushes (average velocity around $4.7\,\mathrm{m/s}$) were $-0.0984 \pm 0.00788\,\mathrm{m/s}^2$ and $-0.126 \pm 0.00359\,\mathrm{m/s}^2$, respectively.

B. Recovery phase analysis

For relaxed-pace propulsion, there was an overestimation for both the straights and turns (see Figure 5). This overestimation was higher for the turns than for the straights. On average the predictions for the straights were $12.5\,\%$ (set 1) and $4.66\,\%$ (set 2) higher than the reference, whereas for the turns the predictions were $17.9\,\%$ (set 1) and $16.9\,\%$ (set 2) higher. Figure 7a shows the instantaneous predicted friction force and power and their corresponding reference signal for the first set. It shows that the friction force and friction power show large deviations from their reference signal.

The sprints only consisted of short pushes. Therefore, no rolling mean could be computed for the sprints (see Figure 7b). Before the actual sprints start, there are some long pushes present where the rolling mean could be computed.

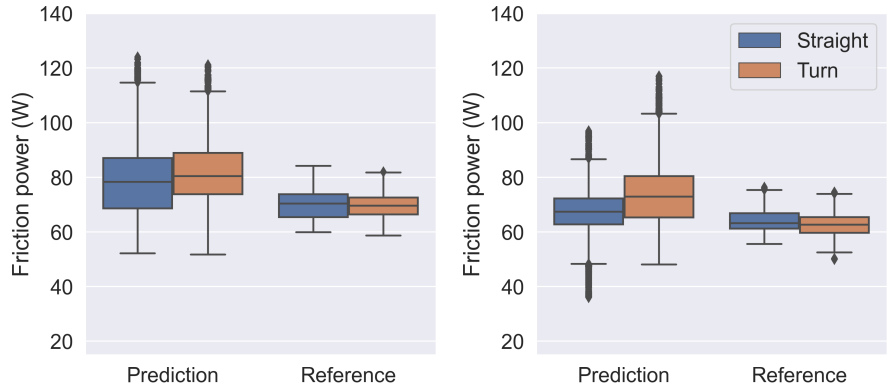

(a) Relaxed-pace, set 1

(b) Relaxed-pace, set 2

Fig. 5: Boxplots of the predicted and reference friction power for the two sets of relaxed-pace propulsion, separated for the turns and straights.

For fast-pace propulsion, there was a general underestimation of the friction power (see Figure 6). Only for the straights in the fourth set, there was an overestimation. There is a large variation in the estimated averages between the different sets, indicating that the average prediction is not consistent. Figure 7c shows the instantaneous friction force and power estimation of the first fast-pace set. It shows that there were not enough long pushes present to produce a continuous rolling mean, resulting in gaps in the prediction signal.

C. Machine learning

The RFR model prediction had an MAE of $3.49 \cdot 10^{-4}$ W, an RMSE of $6.67 \cdot 10^{-4}$ W and an R2 of 1.00. The performance measures of the model per propulsion task are presented in Table I. Figure 8 shows the predicted friction power from the velocity signal by the machine-learning model and the reference power for a small part of the relaxed-pace propulsion data to demonstrate the goodness of fit of the machine-learning model and illustrate the shape of the friction power signal throughout the propulsion cycle. It shows that the variation in friction power is approximately 7.5 W within the propulsion cycle.

TABLE I: Performance measures for the RFR model per type of propulsion task.

	Relaxed-pace	**Sprints**	**Fast-pace**
MAE (W)	$2.28 \cdot 10^{-4}$	$7.20 \cdot 10^{-4}$	$4.21 \cdot 10^{-4}$
RMSE (W)	$3.39 \cdot 10^{-4}$	$1.26 \cdot 10^{-3}$	$7.70 \cdot 10^{-4}$
R2 (-)	1.00	1.00	1.00

IV. Discussion

The aim of this study was to investigate whether it is possible to estimate friction power from IMU data during manual wheelchair propulsion. Two approaches were implemented. Firstly,

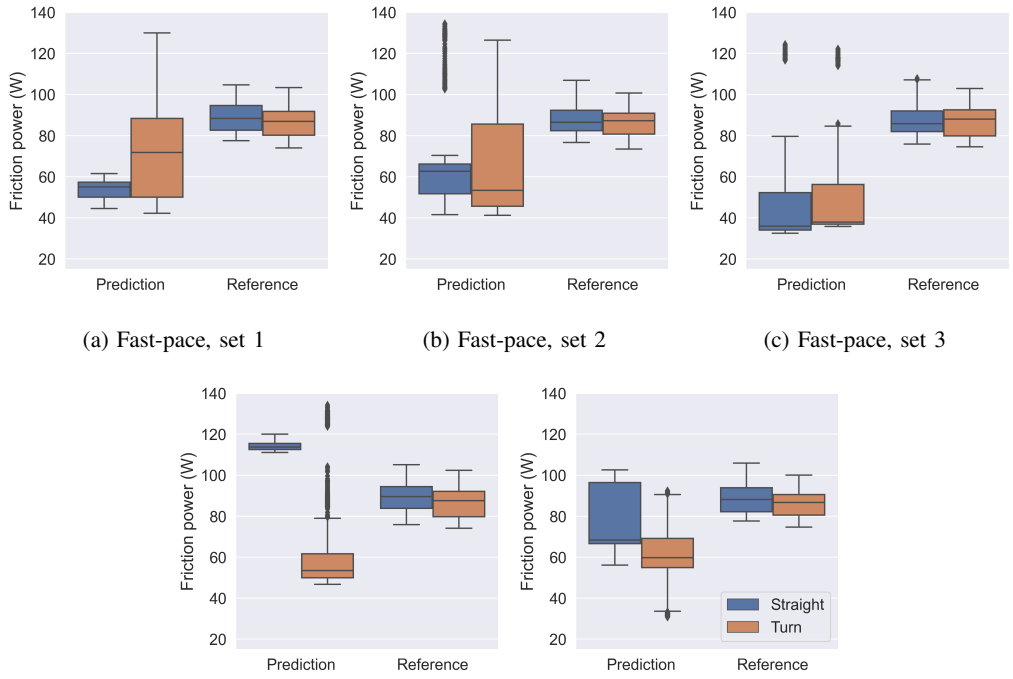

(a) Fast-pace, set 1 (b) Fast-pace, set 2 (c) Fast-pace, set 3

(d) Fast-pace, set 4 (e) Fast-pace, set 5

Fig. 6: Boxplots of the predicted and reference friction power for the five sets of fast-pace propulsion.

a recovery phase analysis was implemented, which estimates the deceleration in the recovery phase to estimate friction forces and power. Secondly, a Random Forest Regressor algorithm was trained to predict friction power based on velocity data.

A. Recovery phase analysis

Results indicate that the recovery phase analysis in which the recovery phase is considered a coast-down period is not a viable method to determine friction power. First of all, this approach can only be used when long pushes are frequently present. However, the results show that this was not the case during sprints and fast-pace propulsion. On top of this, even when long pushes were frequently present, which was mainly the case for relaxed-pace propulsion, the friction power estimation was not accurate enough for use by professional athletes. Firstly, there was a significant mean overestimation of the friction power. Secondly, the instantaneous prediction showed too much variation, leading to large errors in the instantaneous friction power estimation.

The recovery phases could be selected using an automated algorithm. However, in some cases, this algorithm still resulted in the selection of faulty recovery phases. Sometimes, this even led to a fitted acceleration instead of a deceleration. Moreover, the algorithm sometimes selected a segment in which braking occurred. When looking at the whole measurement, it was found that the selection of faulty recovery phases with unrealistic fitted decelerations mainly occurred at lower velocities (below 2.5 m/s). These velocities were not analysed in this study

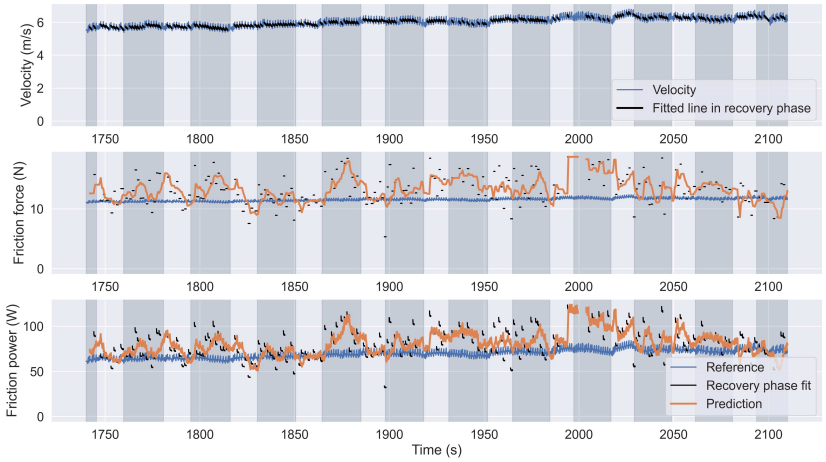

(a) Relaxed-pace

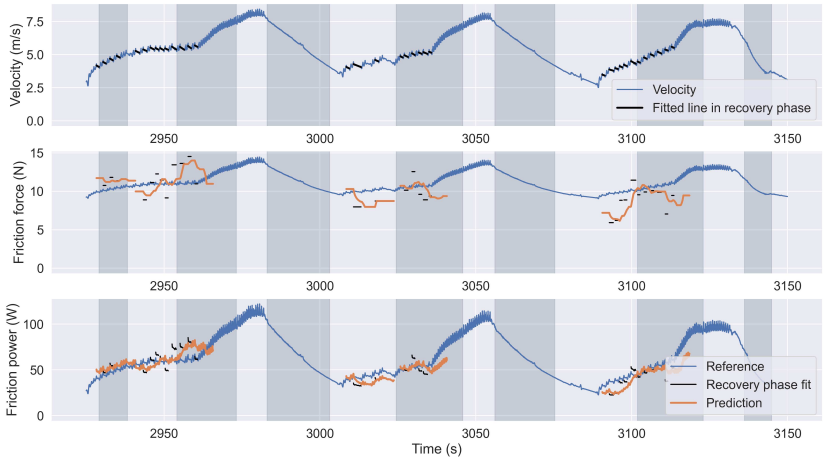

(b) Sprints

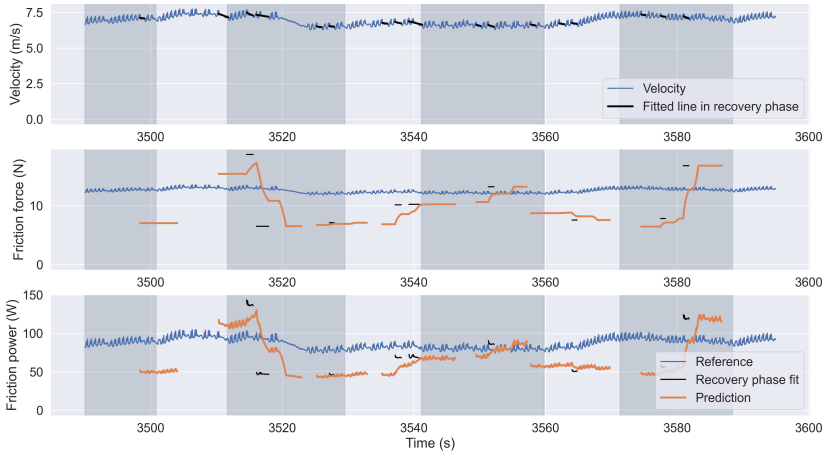

(c) Fast-pace

Fig. 7: Velocity, estimated and reference friction force and friction power for a relaxed pace, sprints and fast pace. The black lines represent the fits in the recovery phase. The orange line is the 5-second rolling mean of the black line which forms the final prediction.

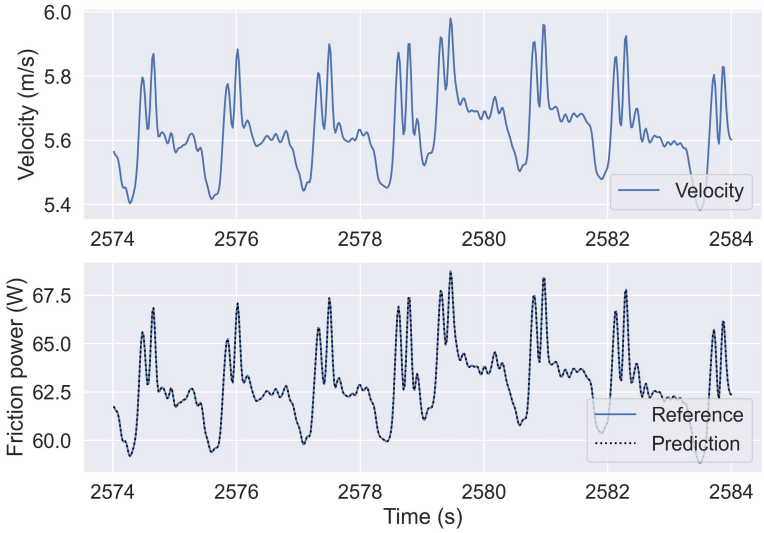

Fig. 8: Velocity, reference power and predicted friction power by the RFR for a few pushes in the test set (relaxed-pace).

and would not occur often in a wheelchair race, but this could be a problem when this analysis would be used for a wheelchair sport in which velocities are lower. To remove the faulty coast-down areas, some extra checks were implemented after the automated algorithm was implemented (removing too short and long recovery phases and removing unrealistically high or low deceleration values). Furthermore, Figure 3 shows that the selection of the beginning of the coast-down area was inconsistent: in some cases, the first peak was selected and in some cases, the second peak was selected. This happens because the algorithm simply selects the peak that is highest and this varies. Thus, the automated selection of the recovery phase was also not completely flawless.

For the relaxed-pace propulsion, the prediction of friction power was slightly higher for the turns than for the straights. It is indeed expected that there is a higher rolling resistance in turns: In turns, there is a centripetal force directed towards the centre of the turn. This force is counteracted by a lateral force which causes a lateral deformation of the tyre. This increased deformation of the tyre increases the rolling resistance loss in turns [21]. In some instances of the relaxed-pace data, it was seen that the velocity is slightly higher on the straights as compared to the surrounding turns, supporting this assumption. Often the velocity was not visibly lower in the turns than on the straights. In that case, it makes sense that the friction power would be higher in the turns as the velocity is similar but there is a higher friction force. However, this higher rolling resistance in the turns was not taken into account when determining the reference friction power.

A possible explanation for the inaccurate results is that the recovery phase is in fact not a perfect coast-down area. The assumption made in a coast-down test is that there is no applied force to the wheelchair. Whereas there is no applied force by the hands, there is trunk movement and movement of the arms which cause forces to be applied to the wheelchair seat. When rotating the trunk forwards or moving the arms forwards, the wheelchair is pushed backwards and vice versa. In the first half of the recovery phase, the trunk still rotates forwards and we

see a slight reduction in the velocity of the wheelchair (see Figure 3). At the end of some of the selected recovery phases, we see that even though the trunk hardly moves, there is an increase in the velocity at the end of the recovery phase. This could be explained by the arms moving backwards to prepare for the next push. Since the athlete's technique will not be perfectly consistent, these influences will also differ for each push. If all these movements were modelled, it should be possible to quantify their effects and get a more accurate result using this analysis. However, this would make the analysis significantly more complex.

B. Machine learning

The machine-learning approach was successful in accurately estimating friction power (R2 = 1.00) from the linear velocity of the wheelchair. This shows that a model can be successfully trained for a specific athlete-wheelchair combination on a specific surface and used to predict the power of the specific athlete-wheelchair combination for unseen IMU data.

In order to train an accurate model, the data of only two IMUs was needed: one on the wheel and one on the frame. From the wheel IMU, the gyroscope data around the wheel axis is required. The gyroscope data of the frame IMU around its vertical axis is needed to correct the wheel IMU measurement for frame rotations.

To the knowledge of the author, no other papers have been published that use a machine-learning approach to estimate the friction power of a wheelchair athlete. However, since the machine-learning model results accurately follow the reference power which is determined from coast-down tests, it is useful to compare the friction coefficients from the coast-down tests to those in other literature to validate the results. Fuss [22] reported μ_R values of 0.0104, 0.0116 and 0.0117, and $C_\mathrm{D}A$ values of $0.1262-0.1358\,\mathrm{m}^2$, $0.1385-0.1445\,\mathrm{m}^2$ and $0.1234-0.1352\,\mathrm{m}^2$ for three different athletes on a granulated rubber track. They also determined these values using a coast-down test. However, Forte et al. [23] reported higher $C_\mathrm{D}A$ values of $0.24\,\mathrm{m}^2$ (recovery phase), $0.33\,\mathrm{m}^2$ (release phase) and $0.41\,\mathrm{m}^2$ (catch phase). These were determined using CFD software. In this paper, μ_R was 0.0102 ± 0.00101 and $C_\mathrm{D}A$ was $0.136 \pm 0.0293\,\mathrm{m}^2$, matching the results of Fuss, but not those of Forte et al. The reason for this might be that the non-linear least-square fit is sensitive to the initial guess and therefore, prone to errors. However, as CFD is sensitive to uncertainties as well, it remains unknown which values are correct.

The present study shows that a machine-learning model is a promising approach to estimating friction power during propulsion without the need to previously determine the friction coefficients with time-consuming methods such as a coast-down test. However, coast-down tests are still required to compute the reference friction power which is needed for training. It remains to be seen if the current model also works for unseen subjects and surfaces. If this is not the case and the model only works for one subject and surface, there is no benefit of this approach over the one used to determine the reference power since both require a coast-down test. Nevertheless, suppose the machine-learning model is able to predict the friction power for unseen subjects and surfaces. This would mean it can predict the power of a subject and surface without the need for a coast-down test for this specific subject and surface. This would mean that an athlete does not need to train a personalised model. Moreover, the model would be able to account for changes in the surface during training which often occur in para-triathlons and marathons without the need for a coast-down test for each surface.

The prediction of friction power can be used to estimate the propulsion power of the athlete, which is the power metric that is interesting for coaches and athletes. To determine the propul-

sion power from the friction power, the power equation needs to be solved (Equation 1). Since only flat surfaces are considered, P_{g} is zero. Hence, the propulsion power is equal to the sum of the friction power (P_{f}) and the kinetic power (P_{kin}). The kinetic power can be determined as described in Equation 1 ($P_{\mathrm{kin}} = mav$).

However, the instantaneous propulsion power is not practical for coaches and athletes. Because of the inevitable cyclic upper body movement in wheelchair propulsion, the acceleration signal of the wheelchair contains large peaks when measured in the field, which translates to large peaks in the propulsion power. This effect was also found by Pelland-Leblanc et al [1]. These peaks hardly relate to the performance of the athlete, but rather to the cyclic chair motion.

Therefore, the instantaneous signal should be converted to a more useful signal for coaches and athletes by filtering out these peaks. One way to reduce these peaks is by strongly filtering the acceleration that is used to compute the kinetic power so that the cyclical accelerations due to the chair movement are removed from the acceleration signal. This would mean that the acceleration that is used to compute the kinetic power should remain zero when the wheelchair is being propelled at an overall constant velocity. Another way to possibly reduce these cyclic accelerations and get a more practical signal would be by looking at the centre of mass motion instead of the wheelchair motion [1]. Another approach to removing the cyclic peak values is by averaging the power over certain time intervals. The 5-second average power is for example often used as a metric in the Wingate Anaerobic Test in which an athlete pedals for 30 seconds at maximum speed against a constant resisting force [24]. Such a time frame still allows the coach and athlete to know how the power changes throughout the training or game without being perturbed as much by the upper body motion.

Although the machine-learning model can accurately predict the reference power, there are some limitations to this study. Based on these limitations some recommendations for future studies can be made.

Firstly, is important to note that the reference power that was used to train the model is also just an estimation and no golden standard. During the coast-down test, the athlete sits as still as possible. However, during actual propulsion, the athlete is moving which causes more friction. This means that the reference power used in this paper was an underestimation of the actual friction power. Since the machine-learning model was trained on this reference power, the machine-learning model also has this underestimation. On top of this, when conducting the least-squares fit to find the coefficients from the coast-down tests, it was concluded that the results depended highly on the initial guess and thus are prone to errors. This also leads to uncertainty in the reference friction power. Moreover, the higher rolling resistance in the turns because of higher tyre deformation due to lateral forces was not taken into account in the prediction of the reference power. However, since the exact relation is not known, this would be difficult to implement. So, even though the machine-learning model can accurately predict the reference friction power, it might not be a perfect prediction of the actual friction power.

Secondly, data from only one subject on one surface was used to train and test the model. This could also explain the high accuracy of the model. Since only intra-subject validation was used, it remains unclear if the current model can predict the friction power of unseen athletes and surfaces. However, it is expected that because only one subject and surface were used (and thus the model was trained for a fixed μ_{R} and $C_{\mathrm{D}}A$), the model was overfitted to this specific subject and surface. Consequently, inter-subject validation of the model is still required by testing the current model on an unseen subject and/or surface in future research.

If it is found that the current model does not work for unseen subjects and surfaces, it is recommended a model be trained for multiple subjects and surfaces, but also other conditions affecting friction forces such as tyre pressure. It is expected that this would produce a model that is more robust to varying circumstances. Furthermore, the model could be expanded by training it for variations in slope and wind, since these conditions can also vary when racing in a triathlon or marathon and influence friction power and propulsion power.

V. Conclusion

Machine learning is a more promising approach to estimating friction power from IMU propulsion data than the recovery phase analysis approach. However, in order to really benefit trainers and athletes, the model needs to be able to predict friction power for unseen subjects and surfaces. Whether the current machine-learning model can do this should still be determined with inter-subject validation. Otherwise, it is recommended that a machine-learning model is trained for multiple subjects and a variation in conditions affecting friction force (surface, tyre pressure, wind, slope) to achieve a more robust model.

References

[1] J.-P. Pelland-Leblanc, F. Martel, È. Langelier, C. Smeesters, F. Berrigan, J. Laroche, and D. Rancourt, "Instantaneous power measurement in wheelchair racing," in *37th Annual Meeting of the American Society of Biomechanics*, 2013.

[2] V. G. de Vette, D. Veeger, and M. P. van Dijk, "Using wearable sensors to estimate mechanical power output in cyclical sports other than cyclingâa review," *Sensors*, vol. 23, no. 1, p. 50, 2022.

[3] T. Rietveld, B. S. Mason, V. L. Goosey-Tolfrey, L. H. van der Woude, S. de Groot, and R. J. Vegter, "Inertial measurement units to estimate drag forces and power output during standardised wheelchair tennis coast-down and sprint tests," *Sports biomechanics*, pp. 1–19, 2021.

[4] Y. Vanlandewijck, D. Theisen, and D. Daly, "Wheelchair propulsion biomechanics," *Sports medicine*, vol. 31, no. 5, pp. 339–367, 2001.

[5] L. Van der Woude, H. Veeger, A. Dallmeijer, T. Janssen, and L. Rozendaal, "Biomechanics and physiology in active manual wheelchair propulsion," *Medical engineering & physics*, vol. 23, no. 10, pp. 713–733, 2001.

[6] E. van der Kruk, F. Van Der Helm, H. Veeger, and A. L. Schwab, "Power in sports: a literature review on the application, assumptions, and terminology of mechanical power in sport research," *Journal of biomechanics*, vol. 79, pp. 1–14, 2018.

[7] G. J. van Ingen Schenau and P. R. Cavanagh, "Power equations in endurance sports," *Journal of biomechanics*, vol. 23, no. 9, pp. 865–881, 1990.

[8] T. M. Barbosa, P. Forte, J. E. Morais, and E. Coelho, "Partial contribution of rolling friction and drag force to total resistance of an elite wheelchair athlete," in *Proc. 1st Int. Conf. in Sports Sciences & Technology (Singapore: Institute of Sports Research)*, 2014, pp. 749–53.

[9] T. M. Barbosa, P. Forte, J. E. Estrela, and E. Coelho, "Analysis of the aerodynamics by experimental testing of an elite wheelchair sprinter," *Procedia Engineering*, vol. 147, pp. 2–6, 2016.

[10] T. M. Barbosa and E. Coelho, "Monitoring the biomechanics of a wheelchair sprinter racing the 100 m final at the 2016 Paralympic Games," *European Journal of Physics*, vol. 38, no. 4, p. 044001, 2017.

[11] C. Sauret, P. Vaslin, M. Dabonneville, and M. Cid, "Drag force mechanical power during an actual propulsion cycle on a manual wheelchair," *Irbm*, vol. 30, no. 1, pp. 3–9, 2009.

[12] P. Forte, D. A. Marinho, J. E. Morais, P. G. Morouço, and T. M. Barbosa, "Estimation of mechanical power and energy cost in elite wheelchair racing by analytical procedures and numerical simulations," *Computer Methods in Biomechanics and Biomedical Engineering*, vol. 21, no. 10, pp. 585–592, 2018.

[13] R. De Klerk, R. J. Vegter, M. T. Leving, S. de Groot, D. H. Veeger, and L. H. van der Woude, "Determining and controlling external power output during regular handrim wheelchair propulsion," *JoVE (Journal of Visualized Experiments)*, no. 156, p. e60492, 2020.

[14] R. Van der Slikke, B. Mason, M. Berger, and V. Goosey-Tolfrey, "Speed profiles in wheelchair court sports; comparison of two methods for measuring wheelchair mobility performance," *Journal of Biomechanics*, vol. 65, pp. 221–225, 2017.

[15] T. Rietveld, R. J. Vegter, R. M. van der Slikke, A. E. Hoekstra, L. H. van der Woude, and S. de Groot, "Wheelchair mobility performance of elite wheelchair tennis players during four field tests: Inter-trial reliability and construct validity," *PLoS One*, vol. 14, no. 6, p. e0217514, 2019.
[16] J. Pansiot, Z. Zhang, B. Lo, and G. Yang, "Wisdom: wheelchair inertial sensors for displacement and orientation monitoring," *Measurement Science and Technology*, vol. 22, no. 10, p. 105801, 2011.
[17] M. P. van Dijk, R. M. van der Slikke, R. Rupf, M. J. Hoozemans, M. A. Berger, and D. H. Veeger, "Obtaining wheelchair kinematics with one sensor only? the trade-off between number of inertial sensors and accuracy for measuring wheelchair mobility performance in sports," *Journal of Biomechanics*, vol. 130, p. 110879, 2022.
[18] M. D. Hoffman, G. Y. Millet, A. Z. Hoch, and R. B. Candau, "Assessment of wheelchair drag resistance using a coasting deceleration technique," *American journal of physical medicine & rehabilitation*, vol. 82, no. 11, pp. 880–889, 2003.
[19] R. van der Slikke, M. Berger, D. Bregman, and D. Veeger, "Push characteristics in wheelchair court sport sprinting," *Procedia Engineering*, vol. 147, pp. 730–734, 2016.
[20] X. Jiang, M. Gholami, M. Khoshnam, J. J. Eng, and C. Menon, "Estimation of ankle joint power during walking using two inertial sensors," *Sensors*, vol. 19, no. 12, p. 2796, 2019.
[21] H. Olofson, "Rolling resistance during cornering-impact of lateral forces for heavy-duty vehicles," 2015.
[22] F. K. Fuss, "Influence of mass on the speed of wheelchair racing," *Sports Engineering*, vol. 12, no. 1, pp. 41–53, 2009.
[23] P. Forte, D. A. Marinho, J. E. Morais, P. G. Morouço, and T. M. Barbosa, "The variations on the aerodynamics of a world-ranked wheelchair sprinter in the key-moments of the stroke cycle: A numerical simulation analysis," *PloS One*, vol. 13, no. 2, p. e0193658, 2018.
[24] L. H. van der Woude, D. Drexhage, and H. Veeger, "Peak power production in wheelchair propulsion," *Clinical Journal of Sport Medicine*, vol. 4, no. 1, pp. 14–24, 1994.